Dipole pulse theory: Maximizing the field amplitude from 4π focused laser pulses

Ivan Gonoskov,[1,*] Andrea Aiello,[1,2] Simon Heugel,[1,2] and Gerd Leuchs[1,2]

[1]*Max Planck Institute for the Science of Light, Günther-Scharowsky-Strasse 1, 91058 Erlangen, Germany*

[2]*Institute for Optics, Information and Photonics, University Erlangen-Nürnberg, Staudtstrasse 7/B2, D-91058 Erlangen, Germany*

(Received 2 May 2012; published 29 November 2012)

We present a class of exact nonstationary solutions of Maxwell equations in vacuum from dipole pulse theory: electric and magnetic dipole pulses. These solutions can provide for a very efficient focusing of electromagnetic field and can be generated by 4π focusing systems, such as parabolic mirrors, by using radially polarized laser pulses with a suitable amplitude profile. The particular cases of a monochromatic dipole wave and a short dipole pulse with either quasi-Gaussian or Gaussian envelopes in the far-field region are analyzed and compared in detail. As a result, we propose how to increase the maximum field amplitude in the focus by properly shaping the temporal profile of the input laser pulses with given main wavelength and peak power.

DOI: 10.1103/PhysRevA.86.053836 PACS number(s): 42.25.Bs, 41.20.Jb, 42.79.Bh

I. INTRODUCTION

Strongly focused electromagnetic fields at subwavelength scales are the centerpiece in many areas of fundamental research and technology, such as high-intensity laser physics, high-resolution optical sensing technologies, and other applications [1–4]. At least two characteristics of these focused electromagnetic fields are significant in this context: first, the maximum value of the electric or magnetic field amplitude in the focus region for a fixed total energy of the input radiation, hence the focusing efficiency, and, second, space and time distributions of electric and magnetic fields near the focus. Owing to this, a detailed analysis of the space-time-dependent field solutions of Maxwell equations in the context of strong focusing is required. Such analysis is the main subject of this paper.

The focusing of monochromatic light was widely discussed [3,5–9], and several corresponding solutions were analyzed (see [3,6,9–15] and references therein). It has been demonstrated that the highest focusing effectiveness can be achieved in the so-called 4π focusing case, where the 4π denotes the coverage of the full solid angle by the incident light. Experimentally, this ideal case can be approached either by using several counterpropagating focused pulses [16], one focused beam and a plane mirror [8], or by suitable formed propagating light beams being mode converted into a nearly perfect dipolar shape by a deep parabolic mirror [4,17,18]. In this case, both propagating and evanescent waves occur, pointing out the difference in the cases of weak focusing from narrow solid angles.

It was rigorously proved in Ref. [19] for monochromatic light that the maximum possible field amplitude for given incoming power and frequency (hence the focusing efficiency) can be achieved in the case of converging dipole radiation. Some practical realizations for the focusing of monochromatic light in vacuum were discussed also in Ref. [20], which studied converging mixed (electric and magnetic) dipole radiation for the achievement of the focusing efficiency close to the maximum possible limit. Nevertheless, both the electromagnetic energy density concentration and corresponding focusing efficiency depend on the typical extensions of the field distribution for the given pulse parameters (frequency, average input power, etc.). Near the focus region the length scale of the distribution is proportional to the wavelength. At large distances the extension is determined by the field amplitude decrease in the far-field region, which is proportional to R^{-1}, where R is the distance from the focus point (see [9,21] and references therein).

A fundamentally different situation arises in the case of focusing nonmonochromatic light, such as short-length laser pulses with an arbitrary broadband carrier-envelope spectrum. In terms of focusing efficiency and energy concentration, the previous considerations for monochromatic light fields cannot be applied in a straightforward fashion. This is due to the interference effects between the various frequency modes of the incident field and the nonlinear condition for the fixed total energy or average input power.

It is nevertheless already obvious that the achievable energy concentration is additionally determined by the duration of the input radiation. For short-length pulses, the concentration of energy can be much smaller than in the case of a focused monochromatic field, which decreases as R^{-1} in the far-field region. The pulse length therefore renders an additional parameter in terms of the energy compression inside the near-focus region.

Additional motivation for considering short electromagnetic pulses arises from the fact that the most powerful attainable laser pulses nowadays can have durations which are less than several optical periods [1,2]. Therefore, this study is relevant for the extreme space-time focusing of light (such as superposition of dipole waves), which is important for high-intensity laser physics applications. Please note here that the temporal focusing of light as a superposition of X-shaped waves was introduced in Refs. [22,23].

Summing up, the scenario which has to be analyzed can be stated as following. An exact nonstationary solution of the Maxwell equations in pure vacuum, achieving high focusing efficiency and possessing a finite total energy, should be found. In this respect we consider the sought solution to be of the class of nonmonochromatic converging dipole radiation since it was demonstrated (see [19]) that the monochromatic dipole wave provides for the maximum possible concentration of the electromagnetic energy.

*ivan.gonoskov@gmail.com

In this paper we consider focusing from the full solid angle for the generation of electric and magnetic dipole pulses using exact nonstationary solutions of the Maxwell equations in vacuum. These solutions are obtained from the dipole pulse theory (DPT). In principal, as follows from DPT, particular cases of the electric and magnetic dipole pulses (for example, an electric dipole monochromatic wave) can be obtained using a field expression for an arbitrary radiating dipole [24,25] and the time reversal transformation (see also [26]). As we will demonstrate, however, the general solution has a more compound structure and needs additional consideration for the derivation. To obtain a singularity-free dipole field solutions, we refer to an analog of the idea of Dirac [27] and Wheeler and Feynman [28], where the mixing of retarded and advanced potentials permits us to eliminate the divergence of the self-energy of charged particles. For the derivation of dipole field distributions without singularities, we present a detailed study of the general case within DPT. In addition, we also illustrate a way for an experimental realization. Dipole pulses can be generated in 4π focusing systems such as parabolic mirrors by using radially polarized laser pulses with a certain amplitude profile and plane phase front [4,17,18,29–34]. In this scheme, we have also analyzed the far-field distribution of the input and expressed all the parameters of the dipole pulses via the initial laser pulses parameters.

As we will demonstrate, dipole pulses provide for very efficient focusing of electromagnetic energy and have some remarkable properties. The particular cases of standing monochromatic dipole waves and short dipole pulses with quasi-Gaussian and Gaussian envelopes in the far-field region are analyzed in detail. We also present the increase of the maximum field amplitude in the focus for a shaped dipole pulse in comparison to a quasimonochromatic dipole pulse with the same main wavelength and maximum value of the initial amplitude in the far-field region or with the same peak power at the input. We show that dipole pulses have some definite advantages in comparison to monochromatic dipole waves regarding high-intensity laser physics and particularly regarding the problem of maximizing the field amplitude in the focus (the effect of a sharply shaped dipole pulse).

This article is organized as follows. In Sec. II we present the dipole pulse theory with a general solution for electric and magnetic dipole pulses. In Sec. III we describe a method suited to generate dipole pulses and express the parameters of the generated dipole pulses through the initial laser pulse parameters at the input. In Secs. IV and V we consider the cases of standing dipole waves and short dipole pulses with a quasi-Gaussian envelope in the far-field region (the case of a Gaussian envelope is analyzed partly in Appendix B). The effect of sharply shaped dipole pulses and the corresponding optimization procedure are presented in Secs. VI and VII. Finally, in Sec. VIII we summarize our results.

II. THE DIPOLE PULSE THEORY: GENERAL SOLUTION

In this section we demonstrate a theoretical procedure which allows us to obtain exact analytical solutions of Maxwell equations in vacuum with finite energy (dipole pulses). This procedure is based on a study of the field distribution of an arbitrary radiating electric dipole.

Let us start from the electromagnetic radiation being emitted from a pointlike nonstationary electric dipole (*e*-dipole). As is well known (see, for example, [21,35]), the radiation of the *e*-dipole which is excited by the arbitrary nonstationary dipole moment $\vec{d}(t)$ can be described by means of the Hertz vector $\vec{Z}_d$:

$$\vec{Z}_d = -\frac{\vec{d}(t-\frac{R}{c})}{R}, \tag{1}$$

where R is the distance from the dipole source to the point of observation. From knowing the Hertz vector, the magnetic ($\vec{H}_d$) and electric ($\vec{E}_d$) field distributions for the radiation field can be written as

$$\vec{H}_d = -\frac{1}{c}(\nabla \times \dot{\vec{Z}}_d), \tag{2a}$$

$$\vec{E}_d = -\nabla \times (\nabla \times \vec{Z}_d). \tag{2b}$$

This field describes divergent *e*-dipole radiation together with the self-field of the *e*-dipole. Applying some simple vector operations (see Appendix A), we can obtain from Eqs. (1) and (2) the following analytic expressions for the magnetic and electric field distributions (see also [25]):

$$\vec{H}_d = -\left\{\vec{n} \times \left[\frac{1}{c^2 R}\ddot{\vec{d}}(\tau) + \frac{1}{cR^2}\dot{\vec{d}}(\tau)\right]\right\}, \tag{3a}$$

$$\vec{E}_d = \vec{n} \times \left[\vec{n} \times \frac{1}{c^2 R}\ddot{\vec{d}}(\tau)\right] + \frac{1}{cR^2}\{3\vec{n}[\vec{n}\cdot\dot{\vec{d}}(\tau)] - \dot{\vec{d}}(\tau)\} + \frac{1}{R^3}\{3\vec{n}[\vec{n}\cdot\vec{d}(\tau)] - \vec{d}(\tau)\}, \tag{3b}$$

where $\vec{n} = \nabla R = \vec{R}/R$ is a unit vector along the direction of observation, $\tau = (t - \frac{R}{c})$, and the dot symbol denotes the derivative with respect to t, e.g., $\dot{\vec{d}}(\tau) = \partial\vec{d}(\tau)/\partial t$. This field consists of two parts: a radiated electromagnetic field and a nonradiated field (the self-field of the *e*-dipole). The latter nonradiated part is given by

$$\vec{H}_d^{nr} = 0, \tag{4a}$$

$$\vec{E}_d^{nr} = \frac{1}{R^3}\{3\vec{n}[\vec{n}\cdot\vec{d}(\tau)] - \vec{d}(\tau)\} \tag{4b}$$

and is directly related to the well-known electric field distribution of a single pointlike nonstatic *e*-dipole.

The presence of this field in the distribution, Eq. (3), leads to some fundamental properties for a nonvanishing dipole moment $\vec{d}(\tau)$:

$$W_d = \frac{1}{8\pi}\int \left[\vec{E}_d^2(\vec{R},t) + \vec{H}_d^2(\vec{R},t)\right]dV = \infty, \tag{5a}$$

$$\frac{dW_d}{dt} = \infty, \tag{5b}$$

where W_d is the total energy of the electromagnetic field. The cause of these infinities is the presence of several singularities in the origin of the coordinates. To describe the nature of these singularities in the region $R \approx 0$, we can use the Taylor

expansion:

$$\vec{d}\left(t-\frac{R}{c}\right)=\sum_{n=0}^{\infty}(-1)^n\frac{\vec{d}^{(n)}(t)}{n!}\left(\frac{R}{c}\right)^n = \vec{d}(t)-\frac{\dot{\vec{d}}(t)}{1!}\frac{R}{c}+\frac{\ddot{\vec{d}}(t)}{2!}\frac{R^2}{c^2}-\frac{\dddot{\vec{d}}(t)}{3!}\frac{R^3}{c^3}+\cdots. \tag{6}$$

By substituting from Eq. (6) into Eq. (3) we obtain, in the limit $R\cong 0$,

$$\vec{H}_d\cong-\vec{n}\times\left[\frac{1}{cR^2}\dot{\vec{d}}(t)-\frac{1}{2c^3}\dddot{\vec{d}}(t)+\cdots\right], \tag{7a}$$

$$\vec{E}_d\cong\frac{1}{R^3}\left\{3\vec{n}[\vec{n}\cdot\vec{d}(t)]-\vec{d}(t)\right\} -\frac{1}{2Rc^2}\{3\vec{n}[\vec{n}\cdot\ddot{\vec{d}}(t)]+\ddot{\vec{d}}(t)\}+\frac{2}{3c^3}\dddot{\vec{d}}(t)+\cdots. \tag{7b}$$

We can see from Eq. (7) that the electromagnetic field of an arbitrary radiating dipole includes strong singularities at $R=0$. These lead to the divergence of the electromagnetic energy. From this we can conclude that such a field cannot be generated, in principle, by using laser fields (with finite energy) in vacuum.

To construct a singularity-free solution, we notice that these singularities are generated by the corresponding R dependence of the Hertz vector near $R=0$:

$$\vec{Z}_d=-\frac{\vec{d}\left(t-\frac{R}{c}\right)}{R} =-\frac{1}{R}\sum_{n=0}^{\infty}(-1)^n\frac{\vec{d}^{(n)}(t)}{n!}\left(\frac{R}{c}\right)^n =-\frac{\vec{d}(t)}{R}+\frac{\dot{\vec{d}}(t)}{c}-\frac{R\ddot{\vec{d}}(t)}{2c^2}+\cdots. \tag{8}$$

To solve this problem we refer to ideas of Dirac [27] and Wheeler and Feynman [28] (see also [36] and references therein), where the authors proposed to use superpositions of retarded and advanced potentials in order to eliminate the divergence of the self-energy of charged particles. In our case, we have the divergence of a radiating dipole field at the origin, which is related to the singularity of its Hertz vector. To obtain the required singularity-free solutions, we propose to consider a linear combination of exact solutions of linear Maxwell equations and to apply transformations to it, under which Maxwell equations remain invariant. One of the transformations, under which the Maxwell equations remain invariant, is the time-reversal transformation (see also [21]):

$$t\to-t,\quad\vec{E}\to\vec{E},\quad\vec{H}\to-\vec{H},\quad\vec{Z}\to\vec{Z}. \tag{9}$$

There exist two specific cases regarding the symmetry of the dipole moment $\vec{d}(\tau)$ under the time-reversal transformation equation (9): (1) $\vec{d}(\tau)$ for even functions and (2) $\vec{d}(\tau)$ for odd functions.

(1) $\vec{d}(\tau)=\vec{d}(-\tau)$. In this case we have

$$\vec{Z}_d=-\frac{\vec{d}(t-\frac{R}{c})}{R}=-\frac{\vec{d}_0}{R}g(t)+\frac{\dot{\vec{d}}(t)}{c}+\cdots, \tag{10a}$$

$$\vec{Z}_d^{-t}=-\frac{\vec{d}(t+\frac{R}{c})}{R}=-\frac{\vec{d}_0}{R}g(t)-\frac{\dot{\vec{d}}(t)}{c}+\cdots, \tag{10b}$$

where $\vec{Z}_d^{-t}$ is obtained from $\vec{Z}_d$ by using time-reversal transformation equation (9). It follows then from Eq. (10) that

$$\vec{Z}_d-\vec{Z}_d^{-t}=-\frac{\vec{d}\left(t-\frac{R}{c}\right)}{R}+\frac{\vec{d}\left(t+\frac{R}{c}\right)}{R} \tag{11}$$

gives us an exact nontrivial singularity-free solution of the Maxwell equations.

(2) $\vec{d}(-\tau)=-\vec{d}(\tau)$. In this case we have

$$\vec{Z}_d=-\frac{\vec{d}(t-\frac{R}{c})}{R}=-\frac{\vec{d}_0}{R}g(t)+\frac{\dot{\vec{d}}(t)}{c}+\cdots, \tag{12a}$$

$$\vec{Z}_d^{-t}=+\frac{\vec{d}(t+\frac{R}{c})}{R}=+\frac{\vec{d}_0}{R}g(t)+\frac{\dot{\vec{d}}(t)}{c}+\cdots. \tag{12b}$$

Again the combination

$$\vec{Z}_d+\vec{Z}_d^{-t}=-\frac{\vec{d}\left(t-\frac{R}{c}\right)}{R}+\frac{\vec{d}\left(t+\frac{R}{c}\right)}{R} \tag{13}$$

gives us an exact nontrivial singularity-free solution of the Maxwell equations.

Let us now consider the most general case, namely, $\vec{d}(\tau)$ being neither an even nor an odd function of τ. Then we can use the expansion

$$\vec{d}(\tau)=\vec{d}_e(\tau)+\vec{d}_o(\tau), \tag{14}$$

where $\vec{d}_e(\tau)=\frac{1}{2}[\vec{d}(\tau)+\vec{d}(-\tau)]$ is an even vector function and $\vec{d}_o(\tau)=\frac{1}{2}[\vec{d}(\tau)-\vec{d}(-\tau)]$ is an odd vector function. From this equation and using Eqs. (11) and (13), we can obtain the required solution as a linear combination of exact Maxwell equation solutions. The corresponding Hertz vector is the following:

$$\vec{Z}=-\frac{\vec{d}\left(t-\frac{R}{c}\right)}{R}+\frac{\vec{d}\left(t+\frac{R}{c}\right)}{R}. \tag{15}$$

It is important to note that this solution cannot be simply obtained from Eq. (3) by applying the time-reversal transformation to arbitrary dipole moment $\vec{d}(\tau)$. To be more precise, any linear combinations of the fields from Eq. (3) and the time reversal fields [which can be obtained by using time reversal transformation in Eq. (3)] can still include singularities. Nevertheless we have obtained the Hertz vector equation (15), which gives us the required solution for an arbitrary vector function $\vec{d}(\tau)$.

We would like also to note that the solution to Eq. (15) can be simply obtained from Eq. (1) either by mixing retarded and advanced Hertz vectors or by using the following transformation:

$$t\to t,\quad R\to-R. \tag{16}$$

We stress here, however, that although both transformations, Eqs. (9) and (16), finally lead to the same expressions for the field distributions, Eq. (16) just amounts to an "empirical" rule, while Eq. (9) constitutes the basis for a rigorous proof.

Finally, from Eqs. (2) and (15) (see also Appendix A), the general, exact, and singularity-free solution for the electromagnetic field of an *e*-dipole pulse can be obtained in the following form:

$$\vec{H} = -\left\{\vec{n}\times\left[\frac{1}{c^2R}\ddot{\vec{d}}_+(t,R)+\frac{1}{cR^2}\dot{\vec{d}}_-(t,R)\right]\right\}, \quad (17a)$$

$$\vec{E} = \vec{n}\times\left[\vec{n}\times\frac{1}{c^2R}\ddot{\vec{d}}_-(t,R)\right] + \frac{1}{cR^2}\{3\vec{n}[\vec{n}\cdot\dot{\vec{d}}_+(t,R)]-\dot{\vec{d}}_+(t,R)\} + \frac{1}{R^3}\{3\vec{n}[\vec{n}\cdot\vec{d}_-(t,R)]-\vec{d}_-(t,R)\}, \quad (17b)$$

where $\vec{d}_\pm(t,R)=\vec{d}(t-\frac{R}{c})\pm\vec{d}(t+\frac{R}{c})$ and $\vec{d}(\tau)$ is an arbitrary vector function, hereinafter referred to as the virtual dipole moment. As can be simply verified, Eq. (17) is an exact solution of the Maxwell equations in vacuum, without any dipole charges, for any arbitrary vector function $\vec{d}(\tau)$.

Let us now consider the temporal and spatial distributions of the field in the near-field and far-field regions. As we can see from Eq. (17b) the electric field of the *e*-dipole pulse consists of three parts:

$$\vec{E} = \vec{E}_1 + \vec{E}_2 + \vec{E}_3, \quad (18)$$

where $\vec{E}_1 \propto R^{-1}$, $\vec{E}_2 \propto R^{-2}$, and $\vec{E}_3 \propto R^{-3}$. In the far-field region ($R\to\infty$) $\vec{E}$ is dominated by $\vec{E}_1$. On the other hand, in the near-field region ($R\approx 0$) all the components enact a part. We can use the expansion, Eq. (6), to obtain

$$\vec{H} = -\left\{\vec{n}\times\left[\frac{2}{3}\frac{R}{c^4}\vec{d}^{(4)}(t)+\cdots\right]\right\}, \quad (19a)$$

$$\vec{E} = \frac{4}{3c^3}\dddot{\vec{d}}(t)+\frac{4}{15}\frac{R^2}{c^5}\left\{\vec{d}^{(5)}(t)-\frac{1}{2}\vec{n}[\vec{n}\cdot\vec{d}^{(5)}(t)]\right\}+\cdots \propto \frac{4}{3c^3}\dddot{\vec{d}}(t)+O(R^2). \quad (19b)$$

At $R=0$ these precisions reduce to

$$\vec{H}(0,t) = 0, \quad (20a)$$

$$\vec{E}(0,t) = \frac{4}{3c^3}\dddot{\vec{d}}(t). \quad (20b)$$

From Eq. (17) we can obtain now

$$W = \frac{1}{8\pi}\int(\vec{E}^2+\vec{H}^2)dV = \text{const}, \quad (21a)$$

$$\frac{dW}{dt} = 0, \quad (21b)$$

where W is a total energy of the *e*-dipole pulse. Since W is finite, this field can thus be generated in vacuum by using electromagnetic fields (for example, laser pulses).

The field distribution of magnetic dipole pulse can be obtained from Eq. (17) by using the following rule [21]:

$$\vec{H}^{MD}\leftarrow\vec{E}^{ED}, \quad \vec{E}^{MD}\leftarrow-\vec{H}^{ED}, \quad (22)$$

where the superscripts ED and MD stand for electric and magnetic dipole pulses, respectively. As can be seen, the field of dipole pulses depends on $\vec{n}$, t, and R and upon the virtual dipole moment $\vec{d}(\tau)$, which can be any smooth vector function.

In the following, we will concentrate on the special case of dipole pulses with $\vec{d}(\tau)=\vec{d}_0 g(\tau)$, where the virtual dipole moment $\vec{d}_0$ is an arbitrary constant vector and $g(\tau)$ is an arbitrary *dimensionless* function (driving function). In this case, the general solution can be simplified to the form

$$\vec{H} = -[\vec{n}\times\vec{d}_0]\left[\frac{1}{c^2}\frac{\ddot{g}_+(t,R)}{R}+\frac{1}{c}\frac{\dot{g}_-(t,R)}{R^2}\right], \quad (23a)$$

$$\vec{E} = \frac{\vec{n}\times[\vec{n}\times\vec{d}_0]}{Rc^2}\ddot{g}_-(t,R)+\frac{3\vec{n}(\vec{n}\cdot\vec{d}_0)-\vec{d}_0}{R^3}\times\left[\frac{R}{c}\dot{g}_+(t,R)+g_-(t,R)\right], \quad (23b)$$

where $g_\pm(t,R)=g(t-\frac{R}{c})\pm g(t+\frac{R}{c})$, $\vec{d}_0$ is a virtual dipole moment (arbitrary constant vector), and $g(\tau)$ is an arbitrary function, hereinafter referred to as the driving function.

III. GENERATION OF DIPOLE PULSES

The idea to generate dipolelike pulses by using external electromagnetic fields is based on the uniqueness of the solutions of the Maxwell equations and, particularly for experimental realizations, the proximity of solutions with nearly the same parameters. Of course, the accuracy of such a scheme in real, nonideal systems, can be analyzed either numerically or experimentally [17,29,33,34]. In this section we consider the case of an ideal infinitely large focusing system.

The basic idea is the following: one has an ideal 4π focusing system (a parabolic mirror or several lenses and so on) which is illuminated by an input light beam of suitable spatial, polarization, and temporal shape. Such a shape is determined by the requirement that the electromagnetic field distribution near the focus (near field) of the focusing system will be described by Eq. (23). The amplitude and the polarization of the input beam far from the focus in the far-field region uniquely determine the near-field dipole pulse characteristics for a given focusing system. In that way, we calculate the dipole radiation flowing through a reference sphere having a big radius (much more than the characteristic wavelength) and use the energy conservation law. We assume that the size of the focusing system is much larger than the main wavelength of the dipole pulse radiation.

The field distribution of the *e*-dipole pulse in the far-field region, also known as the Fraunhofer zone, can be obtained from Eq. (23) by neglecting the R^{-2} and R^{-3} terms:

$$\vec{H} \cong \frac{\vec{d}_0\times\vec{n}}{Rc^2}\left[\ddot{g}\left(t-\frac{R}{c}\right)+\ddot{g}\left(t+\frac{R}{c}\right)\right], \quad (24a)$$

$$\vec{E} \cong \frac{[\vec{d}_0\times\vec{n}]\times\vec{n}}{Rc^2}\left[\ddot{g}\left(t-\frac{R}{c}\right)-\ddot{g}\left(t+\frac{R}{c}\right)\right]. \quad (24b)$$

To study the generation procedure, in the case of pulses with finite duration, we can consider the ingoing [proportional to $\ddot{g}(t+R/c)$] and outgoing [proportional to $\ddot{g}(t-R/c)$] radiation parts separately. We can thereby find the field of the initial ingoing laser pulse, which is required in order to generate the particular finite-length dipole pulse, as

follows:

$$\vec{H}_g = \frac{\vec{d}_0 \times \vec{n}}{R_0 c^2} \ddot{g}(\tau_+), \tag{25a}$$

$$\vec{E}_g = -\frac{[\vec{d}_0 \times \vec{n}] \times \vec{n}}{R_0 c^2} \ddot{g}(\tau_+), \tag{25b}$$

where R_0 is the radius of the reference sphere and $\tau_\pm = t \pm R/c$. As can be seen, the field distribution of the dipole pulse in the far-field region, hence on the sphere with the big radius, corresponds to the plane electromagnetic waves propagating opposite to $\vec{n}$ with a certain amplitude depending on the polar angle θ between $\vec{n}$ and the virtual dipole moment $\vec{d}_0$ and the distance R_0. It additionally follows from Eq. (25) that the ingoing laser pulse envelope $f_l(\tau_+)$ is proportional to the second derivative of the driving function: $f_l(\tau_+) \propto \ddot{g}(\tau_+)$.

The only unknown parameter within these equations is the virtual dipole moment $\vec{d}_0$, as R_0 depends on the size of the focusing system. This virtual dipole moment can be expressed in terms of the initial energy W_p of the ingoing laser pulse. For that we can calculate the radiation power per solid angle $d\Omega$ of the ingoing laser pulse in the far-field region,

$$dP_\tau = -(\vec{S} \cdot \vec{n}) R_0^2 d\Omega = \frac{\ddot{g}^2(\tau_+)}{4\pi c^3} [\vec{d}_0 \times \vec{n}]^2 d\Omega$$
$$= \frac{d_0^2 \ddot{g}^2(\tau_+)}{4\pi c^3} \sin^2\theta \sin\theta d\theta d\varphi, \tag{26}$$

and the total radiation power P_τ, denoting the radiated energy per time unit:

$$P_\tau = \int_0^{2\pi} d\varphi \int_0^{\pi} d\theta \, \frac{d_0^2 \ddot{g}^2(\tau_+)}{4\pi c^3} \sin^3\theta = \frac{2 d_0^2}{3c^3} \ddot{g}^2(\tau_+). \tag{27}$$

Finally, we equate the input laser pulse energy W_p, which is equal to the dipole pulse energy, to the integrated power:

$$W_p = \int_{-\infty}^{\infty} P_\tau d\tau_+ = \frac{2 d_0^2}{3c^3} \int_{-\infty}^{\infty} \ddot{g}^2(\tau_+) d\tau_+. \tag{28}$$

In order to extend the integration limits to infinity without taking into account the divergent (outgoing) radiation depending on τ_-, we consider the case of finite dipole pulses and an indefinitely large focusing system. Based on this last formula, we can express the dipole moment d_0 by the initial laser pulse energy W_p for a definite driving function $g(\tau)$.

Let us now consider the spatial distribution of the dipole pulses and the input laser pulses. In what follows, the virtual dipole vector $\vec{d}_0$ will be set parallel to the z axis. Considering Eq. (25), we can propose a way of generating dipole pulses using a parabolic mirror (see also [4,17]). To this end, we need to obtain the parameters of the laser field at the input of the focusing system required for the generation of a dipole pulse, hence the field polarization and the intensity distribution. The principal scheme of the proposed facility is presented in Fig. 1, with the following form of the parabolic mirror:

$$z = \frac{r^2}{4f} - f, \tag{29}$$

where f is the focusing parameter of the mirror (focal length). We can consider the propagation of light inside the focusing system in terms of optical rays if the condition $f \gg \lambda$ is fulfilled, where λ is the characteristic wavelength of radiation. The optical path length from the input to the focus point of each ray, which is parallel to the z axis at the input of such a focusing system, is equal to $R_0 = L + 2f$, where L is the distance from the focus point of the mirror to its edge on the right side in Fig. 1. If $L \gg f$, then the mirror can produce 4π focusing within the superposition of such optical rays with equal optical path length. In this case, for the generation of dipole pulses, we can use laser pulses with plane phase fronts at the input. We assume further that the condition $L \gg f \gg \lambda$ is fulfilled for the generation procedure. From symmetry considerations and with the help of Fig. 1 and Eq. (25), it follows that a radially polarized field at the input is needed. A discussion concerning the generation of such a field can be found in Refs. [18,29,33,34].

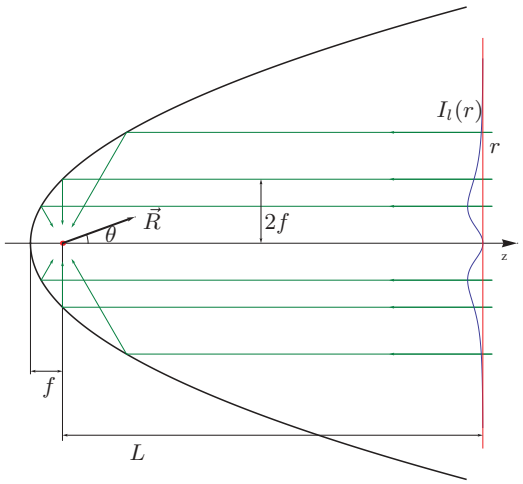

FIG. 1. (Color online) The principal scheme for dipole pulse generation by using a parabolic mirror. Here f is a focusing parameter of the mirror (focal length), L is the distance from the focus (approximate length of the mirror), and $I_l(r)$ is the radial intensity distribution of the input laser radiation.

Now we consider the radial intensity distribution $I_l(r)$ at the input of the parabolic mirror, which is necessary for the generation of dipole pulses, where the subscript l stands for laser. The angular intensity distribution $I_d(\theta)$ is obtained from Eq. (25):

$$I_d(\theta) = I_0 \sin^2\theta, \tag{30}$$

where θ is the polar angle (see Fig. 1) and $I_0 = d_0^2[\ddot{g}(\tau)]^2/4\pi R_s^2 c^3$ [see Eqs. (25) and (26)]. After some simple calculations using Eq. (29) we can write

$$\frac{r}{2f} = \frac{1 + \cos\theta}{\sin\theta}; \tag{31}$$

therefore $\sin\theta = 2p/(p^2+1)$ and $\cos\theta = \pm(p^2-1)/(p^2+1)$, where $p = r/2f$. Using also the relation

$$I_l(r) r dr d\varphi = -I_d(\theta) R_s^2 \sin\theta d\theta d\varphi, \tag{32}$$

we finally obtain

$$I_l(r) = I_0 \frac{R_s^2}{f^2} \frac{4p^2}{(p^2+1)^4}, \tag{33}$$

which can be rewritten in the form

$$I_l(r) = \frac{3}{2}\frac{P_\tau}{\pi f^2}\frac{p^2}{(p^2+1)^4} = \frac{d_0^2 \ddot{g}^2(\tau)}{\pi f^2 c^3}\frac{p^2}{(p^2+1)^4}. \tag{34}$$

The same radial dependence of the intensity distribution was first obtained in Ref. [4]. More cases were analyzed in Ref. [30]. Let us now consider the particular cases of dipole pulses with different driving functions $g(\tau)$, namely, the standing monochromatic dipole wave and finite dipole pulses with quasi-Gaussian and true Gaussian envelopes in the far-field region.

IV. STANDING MONOCHROMATIC DIPOLE WAVE

In order to underline the special advantages of short dipole pulses, we first consider a monochromatic dipole wave which is equivalent to an indefinitely long dipole pulse. Standing monochromatic e-dipole waves are generated by a monochromatic driving function:

$$g(\tau) = \sin(\omega\tau). \tag{35}$$

A similar case was discussed in Refs. [9,35], where the corresponding spatial dependence of the electric field distribution was analyzed. Using the general solution, Eq. (23), we can obtain the field distribution for the monochromatic standing e-dipole wave:

$$\vec{H}(\vec{R},t) = 2\sin(\omega t)(\vec{d}_0 \times \vec{n})\left[-\frac{k^2}{R}\cos(kR) + \frac{k}{R^2}\sin(kR)\right], \tag{36a}$$

$$\vec{E}(\vec{R},t) = 2\cos(\omega t)\left\{\vec{d}_0\left[\left(\frac{k^2}{R} - \frac{1}{R^3}\right)\sin(kR) + \frac{k}{R^2}\cos(kR)\right] + \vec{n}(\vec{n}\cdot\vec{d}_0)\left[\left(-\frac{k^2}{R} + \frac{3}{R^3}\right)\sin(kR) - \frac{3k}{R^2}\cos(kR)\right]\right\}, \tag{36b}$$

where $k = \omega/c = 2\pi/\lambda$. This field is an exact solution of Maxwell equations in vacuum. The corresponding field energy density distribution is shown in Fig. 2. The maximum value of the electric field in the focus, $E_{\max} = |\vec{E}(\vec{R},t)|_{\max} = \underbrace{|\vec{E}_z(\vec{R},t)|}_{R\to 0}$, can be obtained from Eq. (36b) or directly from Eq. (20).

$$E_{\max} = \frac{4}{3}\frac{\omega^3}{c^3}d_0. \tag{37}$$

Using Eq. (27), we can express the virtual dipole moment d_0 as a function of the average input power P:

$$d_0 = \frac{\sqrt{3}}{(2\pi)^2}\frac{\lambda^2\sqrt{P}}{\sqrt{c}}. \tag{38}$$

The average input power is defined as

$$P = \frac{1}{T}\int_0^T P_\tau d\tau, \tag{39}$$

where $T = 2\pi/\omega$ and P_τ is given by Eqs. (27) and (35). Obviously, $P = \frac{1}{2}P_{\text{peak}}$, where P_{peak} is the peak power of the incoming radiation. Finally, we can obtain the expression for the maximum value of the electric field amplitude in a standing e-dipole wave:

$$E_{\max} = \frac{8\pi}{\sqrt{3}}\frac{\sqrt{P}}{\lambda\sqrt{c}}. \tag{40}$$

We can also express this in the following dimensional form:

$$E_{\max} = \frac{8\pi\sqrt{10}\sqrt{10^{-8}\times c/(\text{m/s})}}{100\sqrt{3}} \times 10^8\left(\frac{\text{V}}{\text{m}}\right)\frac{\sqrt{P/\text{W}}}{\lambda/\mu\text{m}} \approx 0.79344\times 10^8\left(\frac{\text{V}}{\text{m}}\right)\frac{\sqrt{P/\text{W}}}{\lambda/\mu\text{m}}. \tag{41}$$

In the same way we can express the maximum value of the magnetic field amplitude near the focus of a standing e-dipole wave through λ and P. This demands, however, solving a transcendent equation for the spatial position of this maximum at $\omega t = \pi/2$ [see Eq. (36a)]. Here, we write only the final approximate result:

$$H_{\max} \approx 0.654 \times E_{\max}. \tag{42}$$

On the contrary, for the case of a standing magnetic dipole wave, we find the maximum value of the magnetic field amplitude in the focus to be equal to the value in Eq. (40) and the maximum value of the electric field to be equal to the value in Eq. (42).

To complete our discussion in this section, we roughly estimate the focusing effectiveness of the monochromatic dipole wave by calculating the corresponding effective focusing spot size δS_{md} and the effective focusing volume V_{md} of the energy

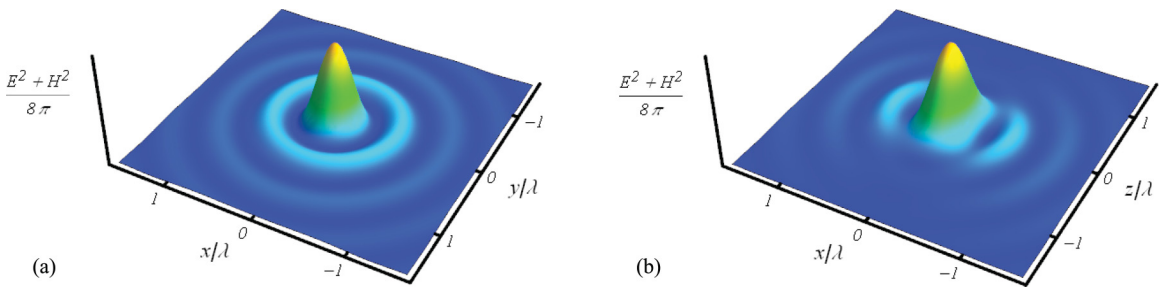

FIG. 2. (Color online) Electromagnetic energy density distribution of the monochromatic e-dipole wave. The energy density ($\omega t = 0$) (a) as a function of transverse coordinates and (b) as a function of the transverse coordinate and the longitudinal one.

density concentration. In the next section, we compare these results to the case of a short dipole pulse.

To estimate the focusing effectiveness we obtain and compare the effective focal spot sizes. We therefore express the energy flux of the monochromatic dipole wave through the average power P and the effective focal spot size δS_{md}:

$$\frac{1}{2}\times\frac{c}{4\pi}E_{\max}^2=\frac{P}{\delta S_{\mathrm{md}}}. \tag{43}$$

Using Eq. (40), we obtain the final expression for the effective spot size of a monochromatic dipole wave:

$$\delta S_{\mathrm{md}}=\frac{3}{8\pi}\lambda^2\approx 0.12\lambda^2. \tag{44}$$

This result demonstrates that the monochromatic dipole wave provides for a much more efficient focusing compared to, for example, a single monochromatic Gaussian beam (corresponding to the case of 2π focusing), which has a significantly bigger focusing spot size. A detailed comparison can be done by using, for example, the results from Refs. [3,10–12,37].

An interesting solution, which leads in some particular cases to the Gaussian beams, was analyzed also in Ref. [38]. This solution does not include singularities and corresponds to the field of higher-order multipoles. Nevertheless, the maximum focusing efficiency of this solution is lower than in our case. As follows from the author's calculations, the thereby found focusing coefficient equals $2\pi\sqrt{5}/\sqrt{3}$ or $2\pi\sqrt{10}/\sqrt{3}$ depending on the polarization. Here we find, for the same coefficient, a value of $8\pi/\sqrt{3}$ [see Eq. (40)]. Similar estimations can also be done for the case of a given set of counterpropagating Gaussian beam pairs, corresponding to the case of 4π focusing (see, for example, [16]). In that case, with an increasing number of counterpropagating Gaussian beams, the difference to the dipole wave case can slightly decrease.

By using the analytical solution (36), we can find also that the effective spatial focusing volume V_{md} of a monochromatic dipole wave (i.e., the electromagnetic energy density concentration volume) is much less than the well-known value λ^3 (see also Fig. 2). To be more precise, we calculate the volume edged by the half height of the energy density concentration (half width at half maximum). In that way, Eq. (36) gives us the characteristic extensions in the longitudinal ($l_{\parallel}\approx 0.58\lambda$) and transversal ($D_{\perp}\approx 0.4\lambda$) directions. From these dimensions, the effective spatial focusing volume V_{md} can be obtained:

$$V_{\mathrm{md}}\leqslant\frac{\pi D_{\perp}^2}{4}l_{\parallel}\approx 0.073\lambda^3. \tag{45}$$

Thus, we can conclude that the monochromatic dipole wave already provides for a very high focusing efficiency. Nevertheless, as we will demonstrate below, short dipole pulses with an appropriate time shape can provide for additional advantages, particularly regarding the maximization of the field amplitude.

V. DIPOLE PULSE WITH A QUASI-GAUSSIAN ENVELOPE IN THE FAR-FIELD REGION

In this part we consider the dipole pulses with a quasi-Gaussian envelope in the far-field region. The field distribution of such a finite pulse can be obtained analytically as a combination of elementary functions at any point in space and time. The case of a Gaussian envelope in the focus is considered in Appendix A. Thus we start with a driving function, which is not equal to the pulse envelope, and consider the case

$$g(\tau)=e^{-a^2\tau^2}\sin(\omega\tau). \tag{46}$$

This type of driving function fulfills the following condition in the far-field region, where $\vec{E}(t)\propto\ddot{g}(t)$:

$$\int_{-\infty}^{\infty}\vec{E}(t)dt=0. \tag{47}$$

The fulfillment of this condition is necessary in order for the pulse to propagate without strong absorption in a media with charged particles; see also [21]. It can be important in the case of the dipole pulse generation within a nonideal vacuum.

The envelope of the input laser pulse for the generation of the dipole pulse with such a driving function is

$$f_l(\tau)\propto\ddot{g}(\tau)=e^{-a^2\tau^2}[-4a^2\omega\tau\cos(\omega\tau)+(4a^4\tau^2-\omega^2-2a^2)\sin(\omega\tau)]. \tag{48}$$

We call such an envelope quasi-Gaussian because, even for short pulses, with durations longer than a few optical periods $a\ll\omega$, and consequently, the envelope is similar to a Gaussian envelope.

The corresponding field distribution for an e-dipole pulse ($a/\omega=0.2$) is shown in Fig. 3. As can be seen from Fig. 3, short dipole pulses provide for a much higher concentration of electromagnetic energy density compared to monochromatic dipole waves (see Fig. 2). Using Eqs. (23) and (46), we can obtain the field distribution analytically at any point in space. As these expressions are too long to be shown here, we limit

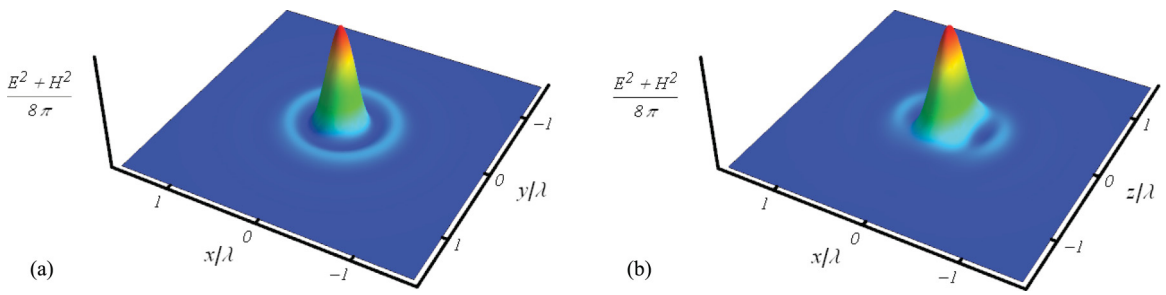

FIG. 3. (Color online) Electromagnetic energy density distribution of an e-dipole pulse with a quasi-Gaussian envelope ($a/\omega=0.2$). The energy density ($\omega t=0$) (a) as a function of transverse coordinates and (b) as a function of the transverse coordinate and the longitudinal one.

ourselves to the field in the focus by using Eq. (20) in order to obtain the maximum value of the electric field:

$$E_z = \frac{4}{3}\frac{d_0}{c^3}e^{-a^2t^2}[(6a^2\omega - 12a^4t^2\omega + \omega^3)\cos(\omega t) + 2a^2t(4a^4t^2 - 3\omega^2 - 6a^2)\sin(\omega t)]. \quad (49)$$

Finally, we can obtain the expression for the maximum value of the electric field amplitude ($\omega t = 0$) for the e-dipole pulse [compare with Eq. (37)]:

$$E_{\max} = E_z(0) = \frac{4}{3}\frac{\omega^3}{c^3}d_0\left(1 + 6\frac{a^2}{\omega^2}\right). \quad (50)$$

Now we need to express the unknown virtual dipole moment through the input laser pulse parameters. Using Eqs. (28) and (46), we can write

$$d_0 = \sqrt{\frac{W_p \times 3c^3}{2N_p}}, \quad (51)$$

where, supposing $a > 0$,

$$N_p = \int_{-\infty}^{\infty}\ddot{g}^2(\tau)d\tau = \frac{\omega^4}{2a}\sqrt{\frac{\pi}{2}}\left[\left(1 + 6\frac{a^2}{\omega^2} + 3\frac{a^4}{\omega^4}\right) - 3\frac{a^4}{\omega^4}e^{-\frac{\omega^2}{2a^2}}\right]. \quad (52)$$

In that way we have

$$d_0 = \frac{\sqrt{W_p \times 3ac^3}}{\omega^2\left(\frac{\pi}{2}\right)^{\frac{1}{4}}\left[\left(1 + 6\frac{a^2}{\omega^2} + 3\frac{a^4}{\omega^4}\right) - 3\frac{a^4}{\omega^4}e^{-\frac{\omega^2}{2a^2}}\right]^{\frac{1}{2}}}. \quad (53)$$

Finally, the field amplitude can be written

$$E_{\max} = \frac{4\omega}{\sqrt{3c^3}}\sqrt{\frac{W_p a}{\sqrt{\pi/2}}}\sqrt{1 + 6\frac{a^2}{\omega^2}} \times \left[1 + \frac{3\frac{a^4}{\omega^4}\left(1 - e^{-\frac{\omega^2}{2a^2}}\right)}{1 + 6\frac{a^2}{\omega^2}}\right]^{-\frac{1}{2}}, \quad (54)$$

or equivalently,

$$E_{\max} = \frac{(8\pi)^{\frac{5}{4}}}{\sqrt{3}}\frac{\sqrt{W_p}}{\lambda^{\frac{3}{2}}}\sqrt{\frac{a}{\omega}\left(1 + 6\frac{a^2}{\omega^2}\right)} \times \left[1 + \frac{3\frac{a^4}{\omega^4}\left(1 - e^{-\frac{\omega^2}{2a^2}}\right)}{1 + 6\frac{a^2}{\omega^2}}\right]^{-\frac{1}{2}}, \quad (55)$$

where $\lambda = 2\pi c/\omega$ is the main wavelength and W_p is the total pulse energy [compare with Eq. (40)]. In a similar way, by additionally solving the transcendent equation for the position, the maximum value of the magnetic field in the e-dipole pulse can be calculated.

Summarizing, we can also estimate numerically the effective focusing volume of energy density concentration V_{dp} for the dipole pulse with the same parameters as in Fig. 3:

$$V_{\text{dp}} \approx 0.032\lambda^3. \quad (56)$$

This result demonstrates that short dipole pulses can provide for more effective focusing (more optimal energy density concentration) compared to a monochromatic dipole wave with the same main wavelength [compare with Eq. (45) and Fig. 2].

VI. OPTIMIZING THE PULSE SHAPE FOR MAXIMIZATION OF THE FIELD AMPLITUDE IN THE FOCUS

Here we consider the problem of how to maximize the field amplitude in the focus by choosing a perfect pulse shape at the input. Under this consideration, we assume that both the pulse energy and the main wavelength are given and limited. From Eq. (40), it is already obvious that infinitely high field amplitudes can be achieved in the case of infinitely small main wavelength. But, as will be demonstrated below, this is not the necessary condition for the maximization problem in the case of nonmonochromatic fields.

Our starting point for finding the solution of the maximization problem is the fact that we have a different time dependence for the field in the focus and in the far-field region. This fact follows directly from DPT [see Eqs. (20) and (25)]. These formulas enable us to express the field amplitude in the focus E_f analytically through the z component of the amplitude in the far-field region E_z [we consider the case $\vec{d}(t) = \vec{d}_0 g(t)$, $\vec{d}_0 = \vec{z}_0 d_0$, $R_0 = R_f$, and $\theta = \pi/2$; see also Fig. 4]:

$$E_f\left(t - \frac{R_f}{c}\right) = \frac{4}{3}\frac{R_f}{c}\dot{E}_z(t). \quad (57)$$

In that way, to maximize the field amplitude in the focus, we need to maximize its first derivative in the far-field region at some moment in time. We therefore do not need to change the main wavelength. Consider, for example, the extreme case where a step function in the envelope of the initial field leads to the generation of a Dirac δ function in the focus (see Fig. 5).

By additionally using formula (27) together with Eqs. (20) and (25) we can obtain an expression for the field amplitude

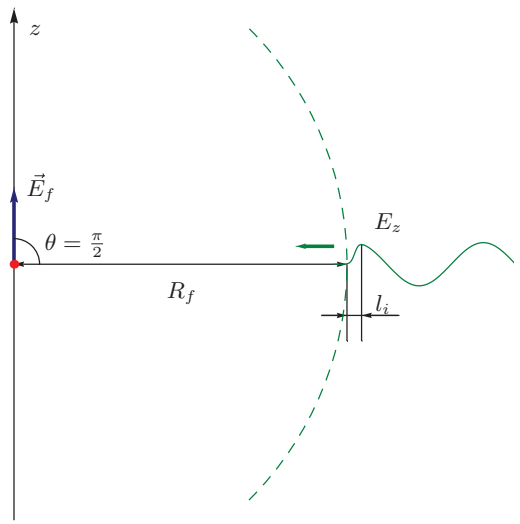

FIG. 4. (Color online) Field distribution of the dipole pulse with a sharp front at some fixed moment of time (green line); l_i is a characteristic pulse buildup length.

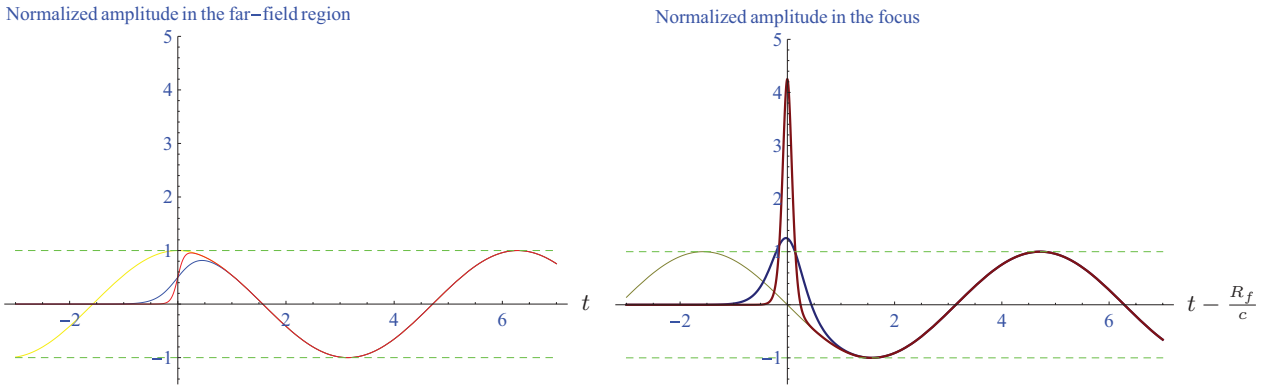

FIG. 5. (Color online) Comparison of the normalized field amplitudes as functions of time (left) in the far-field region and (right) in the focus for a monochromatic *e*-dipole wave (yellow lines) and *e*-dipole pulses with sharp fronts (blue and red lines).

in the focus as a function of the incoming power:

$$E_f\left(t-\frac{R_f}{c}\right)=\pm\left(\frac{8}{3c^3}\right)^{\frac{1}{2}}\frac{d}{dt}[P_\tau(t)]^{\frac{1}{2}}. \tag{58}$$

The field near the sharp front can be approximated as a linear function. We can then obtain from Eq. (57)

$$\mathrm{Max}(E_f)\approx\frac{4}{3}\frac{R_f}{t_i c}E_0=\frac{4}{3}\frac{R_f}{l_i}E_0, \tag{59}$$

where E_0 is a local maximum of E_z, t_i is the characteristic buildup duration, and l_i is the corresponding length (see also Fig. 4). In the case of a monochromatic dipole wave, we can obtain from Eq. (57) the following expression:

$$\mathrm{Max}(E_f)=\frac{8\pi}{3}\frac{R_f}{\lambda}E_0. \tag{60}$$

We can conclude that dipole pulses with sharp edges can give additional advantages regarding the problem of field amplitude maximization. The difference from the monochromatic case can be very high for the case $l_i \ll \lambda$, which can be realized, for example, by using special optical generators [39,40] or by pulse reflection from (or propagation through) a nonlinear medium [41,42].

VII. THE EFFECT OF A SHAPED DIPOLE PULSE AND PHASE OPTIMIZATION

In this section we consider the effect of short or sharply shaped dipole pulses and hence the increase of the maximum field amplitude in the focus from these dipole pulses in comparison to a quasimonochromatic dipole pulse with the same main wavelength and maximum value of initial amplitude in the far-field region or with the same peak power of input pulses. To demonstrate this effect we compare the dipole pulses with different parameters, say with different shapes and carrier envelopes, but the same peak power.

Let us assume that the initial field in the far-field region is determined by two parameters: (1) the envelope $f(t)$ and (2) the phase φ:

$$E(t)=f(t)\sin(\omega t+\varphi). \tag{61}$$

By using Eq. (57), we can write

$$\begin{aligned}&E_f\left(t-\frac{R_f}{c}\right)\\&\quad\propto\dot{f}(t)\sin(\omega t+\varphi)+\omega f(t)\cos(\omega t+\varphi)\\&\quad=\sqrt{\dot{f}^2+\omega^2 f^2}\,\sin\left[\omega t+\varphi+\arcsin\left(\frac{\omega f}{\sqrt{\dot{f}^2+\omega^2 f^2}}\right)\right].\end{aligned} \tag{62}$$

In order to maximize the field amplitude, we first need to find the optimal time t^*, which can be determined from the following condition:

$$t^*:(\dot{f}^2+\omega^2 f^2)\to\mathrm{Max}. \tag{63}$$

After that, we can find the optimal phase φ^* by using the following condition:

$$\omega t^*+\varphi^*+\arcsin\left(\frac{\omega f}{\sqrt{\dot{f}^2+\omega^2 f^2}}\right)=\frac{\pi}{2}. \tag{64}$$

Summarising these results, we conclude, that for shaped dipole pulses [with the form such as in Eq. (61)], under such condition:

$$\exists t^*:(\dot{f}^2+\omega^2 f^2)>\mathrm{Max}(\omega^2 f^2), \tag{65}$$

the effect of the shaped dipole pulse, and hence the increase of the field amplitude above the level of the corresponding monochromatic dipole wave, can be observed. From Eqs. (61)–(64), it follows additionally that if the focused pulse possesses a symmetric envelope (maximum value at $t=0$) and contains at least several optical periods, then $\mathrm{Max}(\dot{f}^2+\omega^2 f^2)=\mathrm{Max}(\omega^2 f^2)$, $t^*=0$, and the optimal phase is $\varphi^*=0$.

VIII. CONCLUSION

We have introduced and analyzed the exact nonstationary solutions of Maxwell equations in vacuum: electric and magnetic dipole pulses, which are obtained from DPT. These pulses can be generated in 4π focusing systems such as parabolic mirrors using radially polarized laser pulses with a suitable radial amplitude profile and a plane phase front at the input. As shown, dipole pulses have at least two remarkable properties: (1) they provide for very good focusing efficiency (regarding the problem of maximizing the field amplitude in the focus) where the characteristic spatial volume of focusing for short pulses is substantially smaller than $0.073\lambda^3$, and (2) they provide also for a very effective separation of the electric and magnetic fields in the focus region. Moreover, we demonstrated that sharply shaped dipole pulses with a given peak power and main wavelength can produce a sharply peaked amplitude of the field in the focus. Also a certain choice of carrier envelope of the shaped dipole pulse at the input allows us to achieve the effect of an increase of the maximum value of the field amplitude in the focus for a shaped dipole pulse in comparison with a quasimonochromatic dipole pulse under the same input conditions, the main wavelength, and peak power in the far-field region. The corresponding optimization procedure is analyzed. All these properties give us the opportunity of using dipole pulses for a number of problems and applications of high-intensity laser physics (see [1] and references therein), namely, charged-particle acceleration, high harmonic generation in the relativistic regime, and electron-positron pair production in vacuum.

ACKNOWLEDGMENT

One of us (I.G.) would like to thank Denis Sych for useful and stimulating discussions.

APPENDIX A

In this appendix, we point out some mathematical formulas and expressions which we use for the derivation of the field distributions, Eqs. (3) and (23). For the derivation of the electric field distribution one can use the well-known formula for an arbitrary vector function $\vec{M}$:

$$\nabla \times [\nabla \times \vec{M}] = \mathrm{grad}(\mathrm{div}\vec{M}) - \Delta\vec{M}, \tag{A1}$$

where $\Delta = \nabla \cdot \nabla$ is the Laplace operator. In order to perform vector operations, we can use the following expressions for a vector function of the form $\vec{F} = \vec{F}(R,t)$:

$$\nabla \times \vec{F} = \vec{n} \times \frac{\partial \vec{F}}{\partial R}, \tag{A2a}$$

$$\mathrm{div}\vec{F} = \vec{n} \cdot \frac{\partial \vec{F}}{\partial R} = \vec{R} \cdot \frac{1}{R}\frac{\partial \vec{F}}{\partial R}, \tag{A2b}$$

$$\mathrm{grad}(\vec{R} \cdot \vec{F}) = \vec{F} + \vec{R}\left(\vec{n} \cdot \frac{\partial \vec{F}}{\partial R}\right). \tag{A2c}$$

Thus, if we have a combination $(t \pm \frac{R}{c})$ in any part of the vector functions used, the corresponding spatial partial derivative ∂R can be replaced by the temporal partial derivative ∂t. Finally, we make use of a simple, well-known formula from vector analysis:

$$\vec{a} - \vec{n}(\vec{n} \cdot \vec{a}) = \vec{n} \times [\vec{a} \times \vec{n}]. \tag{A3}$$

APPENDIX B

Here we present a derivation of the driving function for a dipole pulse with a Gaussian envelope. As follows from Eq. (23), it is enough to obtain the field distribution in any point of space and time. Our goal is to find the driving function $g(t)$ which satisfies the condition

$$\ddot{g}(t) = e^{-a^2t^2}\sin(\omega t). \tag{B1}$$

For that we can find first time integrate of $\ddot{g}(t)$ to obtain

$$\dot{g}(t) = \frac{i\sqrt{\pi}}{4a}e^{-\frac{\omega^2}{4a^2}}\left[\mathrm{erf}\left(at + \frac{i\omega}{2a}\right) - \mathrm{erf}\left(at - \frac{i\omega}{2a}\right)\right], \tag{B2}$$

where $\mathrm{erf}(x)$ is the error function:

$$\mathrm{erf}(x) = \frac{2}{\sqrt{\pi}}\int_0^x e^{-y^2}dy. \tag{B3}$$

Using the simple formula

$$\frac{d}{dx}\left[x\mathrm{erf}(x) + \frac{e^{-x^2}}{\sqrt{\pi}}\right] = \mathrm{erf}(x), \tag{B4}$$

the required driving function can be obtained from Eq. (B2) in the following form:

$$g(t) = \frac{i\sqrt{\pi}}{4a}e^{-\frac{\omega^2}{4a^2}}\left[\left(at + \frac{i\omega}{2a}\right)\mathrm{erf}\left(at + \frac{i\omega}{2a}\right) - \left(at - \frac{i\omega}{2a}\right)\mathrm{erf}\left(at - \frac{i\omega}{2a}\right)\right]. \tag{B5}$$

This real function satisfies (B1) and determines completely the propagation of the dipole pulse with a Gaussian envelope in the far-field region.

[1] G. A. Mourou, T. Tajima, and S. V. Bulanov, Rev. Mod. Phys. **78**, 309 (2006).
[2] G. Mourou and T. Tajima, Science **331**, 41 (2011).
[3] H.-S. Chon, G. Park, S.-B. Lee, S. Yoon, J. Kim, J.-H. Lee, and K. An, J. Opt. Soc. Am. A **24**, 60 (2007).
[4] N. Lindlein, R. Maiwald, H. Konermann, M. Sondermann, U. Peschel, and G. Leuchs, Laser Phys. **17**, 927 (2007).
[5] P. Debye, Ann. Phys. (Leipzig) **30**, 57 (1909).
[6] M. Born and E. Wolf, *Principles of Optics* (Cambridge University Press, Cambridge, 1999).
[7] S. Quabis, R. Dorn, M. Eberler, O. Glöckl, and G. Leuchs, Opt. Commun. **179**, 1 (2000).
[8] E. Mudry, E. Le Moal, P. Ferrand, P. C. Chaumet, and A. Sentenac, Phys. Rev. Lett. **105**, 203903 (2010).

[9] V. Dhayalan, Ph.D. dissertation, University of Bergen, Bergen, Norway, 1996.
[10] Y. Li and F. Yu, Opt. Commun. **70**, 1 (1989).
[11] P. Varga and P. Török, Opt. Commun. **152**, 108 (1998).
[12] P. J. Cronin, P. Török, P. Varga, and C. Cogswell, J. Opt. Soc. Am. A **17**, 1556 (2000).
[13] N. Narozhny and M. Fofanov, J. Exp. Theor. Phys. **90**, 753 (2000).
[14] H. P. Urbach and S. F. Pereira, Phys. Rev. Lett. **100**, 123904 (2008).
[15] H. P. Urbach and S. F. Pereira, Phys. Rev. A **79**, 013825 (2009).
[16] S. S. Bulanov, V. D. Mur, N. B. Narozhny, J. Nees, and V. S. Popov, Phys. Rev. Lett. **104**, 220404 (2010).
[17] G. Leuchs, K. Mantel, A. Berger, M. Konermann, M. Sondermann, U. Peschel, N. Lindlein, and J. Schwider, Appl. Opt. **47**, 5570 (2008).
[18] N. Davidson and N. Bokor, Opt. Lett. **29**, 1318 (2004).
[19] I. M. Bassett, Opt. Acta **33**, 279 (1986).
[20] C. J. R. Shepard and K. G. Larkin, J. Mod. Opt. **41**, 1495 (1994).
[21] L. D. Landau, and E. M. Lifshitz, *The Classical Theory of Fields* (Pergamon Press, Oxford, 1987).
[22] A. M. Shaarawi, I. M. Besieris, and T. M. Said, J. Opt. Soc. Am. A **20**, 1658 (2003).
[23] M. Zamboni-Rached, A. M. Shaarawi, and E. Recami, J. Opt. Soc. Am. A **21**, 1564 (2004).
[24] O. D. Jefimenko, Am. J. Phys. **60**, 899 (1992).
[25] W. J. M. Kort-Kamp and C. Farina, Am. J. Phys. **79**, 111 (2011).
[26] J. de Rosny and M. Fink, Phys. Rev. A **76**, 065801 (2007).
[27] P. A. M. Dirac, Proc. R. Soc. London, Ser. A **5**, 148 (1938).
[28] J. A. Wheeler and R. P. Feynman, Rev. Mod. Phys. **15**, 157 (1945).
[29] R. Dorn, S. Quabis, and G. Leuchs, Phys. Rev. Lett. **91**, 233901 (2003).
[30] M. Sondermann, N. Lindlein, and G. Leuchs, arXiv:0811.2098.
[31] L. E. Helseth, Phys. Rev. E **72**, 047602 (2005).
[32] L. E. Helseth, J. Opt. **12**, 035705 (2010).
[33] S. Quabis, R. Dorn, M. Eberler, O. Glöckl, and G. Leuchs, Appl. Phys. B **72**, 109 (2001).
[34] S. Quabis, R. Dorn, and G. Leuchs, Appl. Phys. B **81**, 597 (2005).
[35] C. Cohen-Tannoudji, J. Dupont-Roc, and G. Grynberg, *Photons and Atoms* (Wiley, New York, 1989), Exercise CI.6, p. 71.
[36] T. Erber, Fortschr. Phys. **9**, 343 (1961).
[37] S. Orlov and U. Peschel, Phys. Rev. A **82**, 063820 (2010).
[38] A. M. Fedotov, Laser Phys. **19**, 214 (2009).
[39] D. D. Yavuz, Science **331**, 1142 (2011).
[40] H.-S. Chan, Z.-M. Hsieh, W.-H. Liang, A. H. Kung, C.-K. Lee, C.-J. Lai, R.-P. Pan, and L.-H. Peng, Science **331**, 1165 (2011).
[41] U. Teubner and P. Gibbon, Rev. Mod. Phys. **81**, 445 (2009).
[42] A. A. Gonoskov, A. V. Korzhimanov, A. V. Kim, M. Marklund, and A. M. Sergeev, Phys. Rev. E **84**, 046403 (2011).